Supplementary data

Target gene	Primer name	Primer sequence (5' - 3')
PCR primers		
DMP19 gene	DMP19-F	5’-GATCCATATGACTGCGCTTACCCTTCC-3’
	DMP19-R	5’-GATAGGATCCTCACGCCTGCCCGATATG-3’
NHTF gene	NHTF-F	5’-GATCCATATGATGGGCAACAAATTGACTCTGC-3’
	NHTF-R	5’-GATAGGATCCAATACCGCTTTCAGACG -3’
NHTF 5’untranslated region	NHTF5’UT-F	5’-GCGCTGTTTCCCAATCTGTCTTGATTTTATCTC-3’
	NHTF5’UT-R	5’-GCGCTTGCTTCCAGATAAATGGTTAAAGTTAAGC-3’
Complementary synthesized oligonucletides for short dsDNA fragments		
Fragment 1 of NHTF 5’ untranslated region	First fragment-F	5’-TGTTTCCCAATCTGTCTTGATTTTATCTCTTTCCTC-3’
	First fragment-R	5’-GAGGAAAGAGATAAAATCAAGACAGATTGGGAAACA-3’
Fragment 2 of NHTF 5’ untranslated region	Second fragment-F	5’-TTGATGTGTGTGTGTTTGGGTGTGGCTGCCGCCACCC-3’
	Second fragment-R	5’-GGGTGGCGGCAGCCACACCCAAACACACACACATCAA-3’
Fragment 3 of NHTF 5’ untranslated region	Third fragment-F	5’-CTTTTTTTTGGCTTTTATGTGAAGTAAAATCCGTAACAGC-3’
	Third fragment-R	5’-GCTGTTACGGATTTTACTTCACATAAAAGCCAAAAAAAAG-3’
Fragment 4 of NHTF 5’ untranslated region	Fourth fragment-F	5’-AAATGCTTAACTTTAACCATTTATCTGGAAGCAA-3’
	Fourth fragment-R	5’-TTGCTTCCAGATAAATGGTTAAAGTTAAGCATTT-3’
25-mer DNA fragment from third fragment with TGTNAN$_{11}$TNACA sequence	Specific-F	5’-TATGTGAAGTAAAATCCGTAACAGC-3’
	Specific-R	5’-GCTGTTACGGATTTTACTTCACATA -3’
25-mer DNA fragment from third fragment without TGTNAN$_{11}$TNACA sequence	Nonspecific-F	5’-ACCCCTTTTTTTTGGCTTTTATGTG -3’
	Nonspecific-R	5’-CACATAAAAGCCAAAAAAAAGGGGT -3’
25-mer DNA fragment from third fragment with mutated *CCC*NAN$_{11}$TNACA sequence	Specific (mutant)-F	5’-TACCCGAAGTAAAATCCGTAACAGC-3’
	Specific (mutant)-R	5’-GCTGTTACGGATTTTACTTCGGGTA -3’

Table S1. PCR primers and complementary synthesized oligonucletides for short dsDNA fragments

Band	Protein name (species)	Acc. No.	MS/mps*	Sequence coverage
a	DNA-directed RNA polymerase subunit beta' [*Neisseria meningitidis* 053442]	YP_001600102	173/14	11%
b	Pyruvate dehydrogenase subunit E1 [*Neisseria meningitidis* MC58]	NP_274360	260/13	18%
c	Molecular chaperone DnaK [*Neisseria meningitidis* Z2491]	YP_002342189	257/14	22%
d	Elongation factor Tu [*Neisseria meningitidis* MC58]	NP_273182	422/16	44%
e	DNA-directed RNA polymerase subunit alpha [*Neisseria meningitidis* MC58]	NP_273226	54/4	12%
f	Hypothetical transcription factor (NHTF) [*Neisseria meningitidis* MC58]	NP_274229	95/6	56%

Table S2. Protein identification by LC-nanoESI-MS/MS

* MS/mps: Mowse Score/matched peptides.

	Theoretical MW[a]	S[b] predicted by HYDROPRO	Observed S from AUC	Predicted MW from SV data	Predicted MW from GF75 column
DMP19 monomer	18.5 kDa	1.99	2.13	17.5 kDa	not seen [c]
DMP19 dimer	37 kDa	3.23	3.6	39.5 kDa	43 kDa
NHTF dimer	26 kDa	2.24	2.2	25.1 kDa	24.5 kDa
DMP19 dimer+NHTF dimer	63 kDa	4.54	4.35	54.8 kDa	74 kDa

Table S3. Sedimentation coefficient results and molecular weight

[a]The theoretical molecular weight is based on the amino acid sequence.

[b]HYDROPRO (1) predicted the S values based on the atomic coordinates model.

[c]DMP19 dimerization is concentration dependent; the monomeric form of DMP19 was not found at the experimental concentration.

Supplementary Figure Legends

Figure S1. Multiple amino acid sequence alignment of 6 XRE transcription factors.

Figure S2. A His-pulldown assay was used to detect interactions between DMP19 and several DNA binding proteins. By using extracted *Neisseria* proteins as prey and N-terminal His10-tagged DMP19 as bait, six *Neisseria* proteins were pulled down by DMP19 (table S1). One of these proteins, NHTF transcription factor, was chosen for further study.

Figure S3. The presence of DMP19 and NTHF in the same shift bands (labeled by *) in BS3 cross-linking study was also confirmed by Western blot analysis using anti-DMP19 and anti-NHTF antibodies, respectively.

Figure S4. Sedimentation velocity (SV) analysis of DMP19/NHTF complex formation by analytical ultracentrifugation. For sedimentation velocity (SV) analysis, all samples were diluted to a suitable concentration (OD 280 absorption between 0.1~0.8) using 20 mM Tris pH 7.2 buffer. Analytical ultracentrifugation was performed at 45000 rpm using a 4-hole AnTi60 rotor at 20 ℃ in a Beckman Optima XL-1 AUC equipped with absorbance optics (OD 280 nm). Data were analyzed using

the with c(s) distribution of the Lamm equation solutions calculated by the program SEDFIT (http://www.analyticalultracentrifugation.com). The SEDFIT parameters were: the buffer density 0.9988 g/ml; buffer viscosity 0.01069 poise; the protein partial specific volumes for each analysis were 0.7313 (DMP19 dimer), 0.7355 (NHTF dimer) and 0.73 (NHTF dimer/DMP19 dimer). The predicted molecular weights of each analysis were also calculated by the same program. (A) 10 μM NHTF. Only the dimeric NHTF form could be found. The predicted molecular weight from the SV data (25.1 kDa) is a good match to the theoretical NHTF dimer molecular weight (26 kDa). (B) 10 μM DMP19. Both monomeric and dimeric forms were found. The molecular weights predicted by SV data matched to the theoretical DMP19 monomer (18.5 kDa) and dimer molecular weights (37 kDa). (C) 7.5 μM DMP19 and 7.5 μM NHTF and (D) 5 μM DMP19 and 10 μM NHTF. A third peak emerged with molecular weight slightly lower than the theoretical molecular weight of the DMP19 dimer/NHTF dimer complex (63 kDa). Since the molecular weight predicted by SEDFIT is affected by the shape and symmetry of the proteins, we used the HYDROPRO program (1) to calculate the theoretical sedimentation coefficient (S value) from the coordinate PDB file of the DMP19 dimer/NHTF dimer binding model. HYDROPRO predicted a theoretical S value of 4.54 which is very close to the S value given by SEDFIT (4.3-4.4). We conclude that the peaks which molecular weights of

54.8 and 53.9 kDa represent the dimeric DMP!9/NHTF complex. A full comparison of the theoretical and observed S values is given in supplementary Table S3.

Figure S5. (A) Superposition of the core structure (α-Helix 1-4) from four XRE transcription factors. NHTF (residues 17-75; blue), restriction-modification controller protein C.BclI (2B5A, residues 5-64; cyan), C.AhdI (1Y7Y, residues 9-67; yellow) and 434 Cro repressor (3Cro, residues 3-54; magenta). The RMSD fit for the 59 equivalent C^{α} atoms from the core structure of NHTF is 0.90 Å for C.BclI, 0.71 Å for C.AhdI and 0.63 Å for 434 Cro repressor. (B) The proposed DNA binding region of the *Neisseria* NHTF transcription factor. The phage 434 CRO/DNA complex structure (magenta) was superimposed with *Neisseria* NHTF transcription factor (blue). In this model of the DNA binding region of NHTF, the positively charged helix α3 of NHTF is the recognition helix that binds to the major groove of DNA.

Figure S6. EMSA results show that only the NHTF 5' untranslated region PCR product was shifted after incubation with NHTF.

Figure S7. The sequence of designed NHTF operon that used in *in situ* gene regulation assay. RBS: ribosome binding site. GFP: green fluorescent protein.

Figure S8. Complementary surface charges of DMP19 and NHTF.

Supplementary References

1. Ortega, A., Amorós, D. and García de la Torre, J. (2011) Prediction of hydrodynamic and other solution properties of rigid proteins from atomic- and residue-level models. *Biophys J,* **101**, 892-898.

Supplementary figures

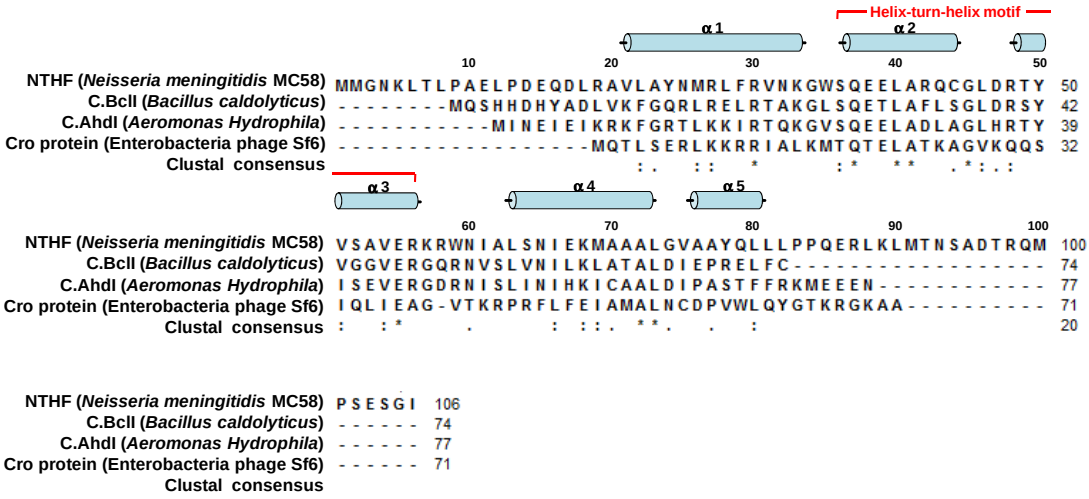

Figure S1

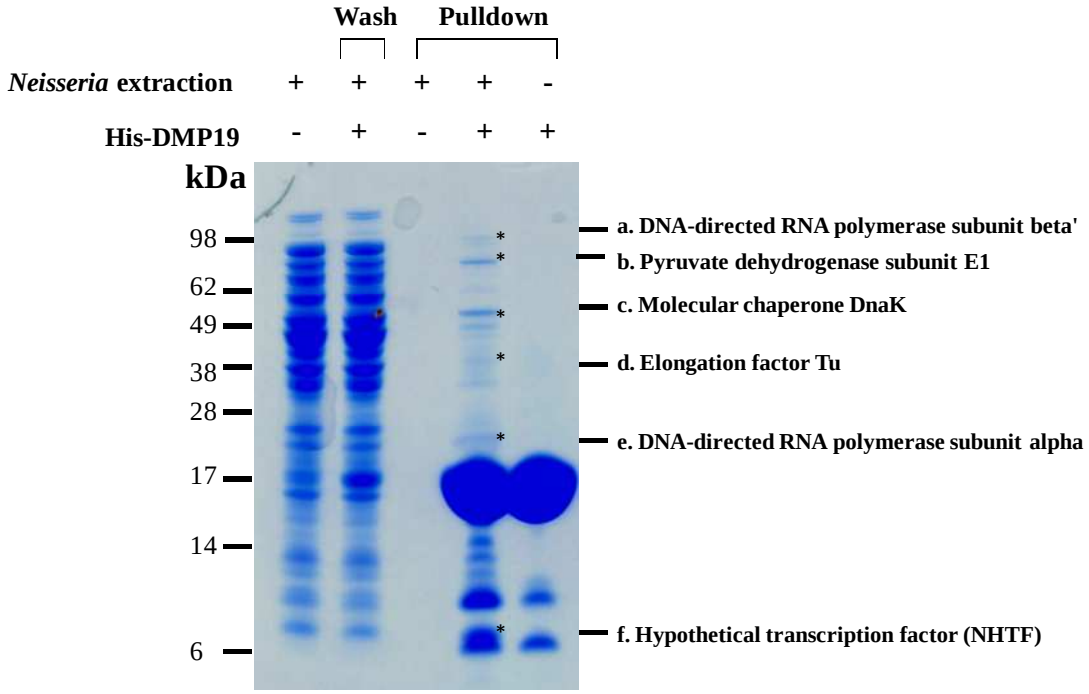
Wash
Pulldown
Neisseria extraction + + + + -
His-DMP19 - + - + +
kDa
98
62
49
38
28
17
14
6
a. DNA-directed RNA polymerase subunit beta'
b. Pyruvate dehydrogenase subunit E1
c. Molecular chaperone DnaK
d. Elongation factor Tu
e. DNA-directed RNA polymerase subunit alpha
f. Hypothetical transcription factor (NHTF)

Figure S2

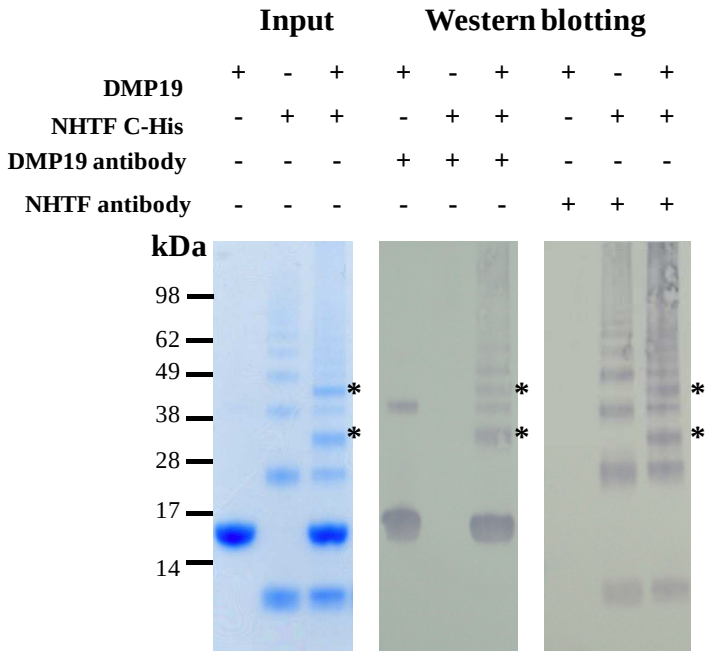
Input
Western blotting
DMP19
NHTF C-His
DMP19 antibody
NHTF antibody
kDa
98
62
49
38
28
17
14

Figure S3

Figure S4 (A)

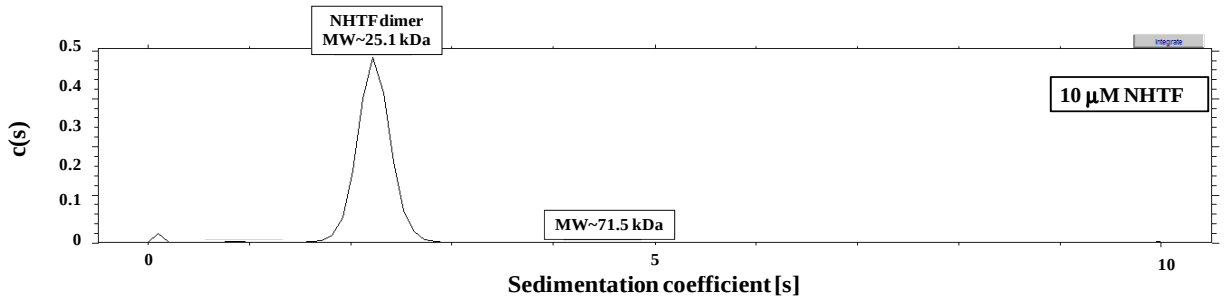

Figure S4 (B)

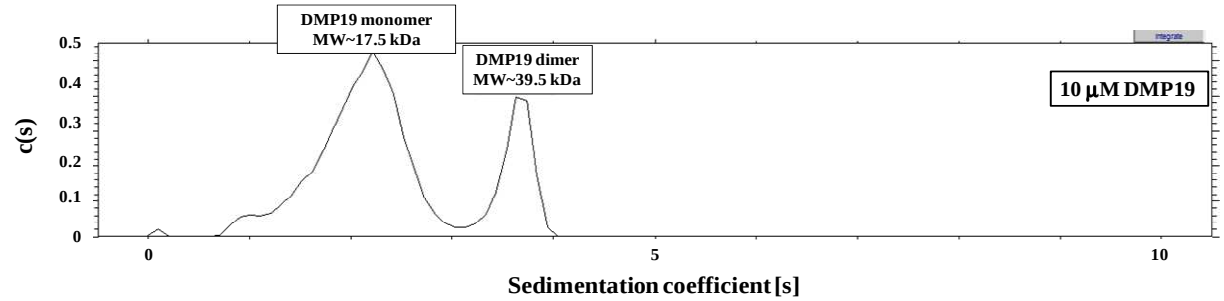

Figure S4 (C)

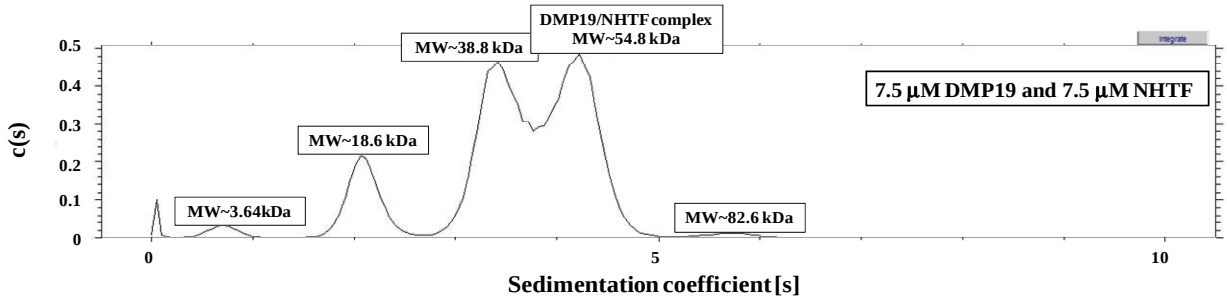

Figure S4 (D)

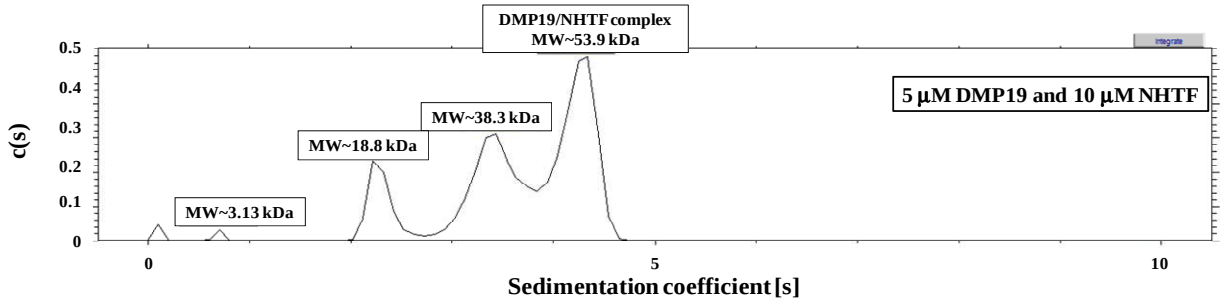

Figure S4

Figure S5 (A)

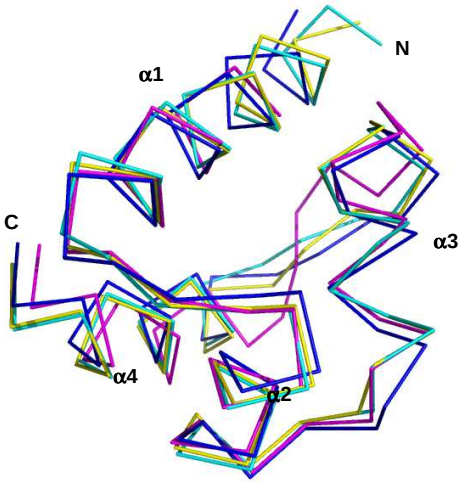

Figure S5 (B)

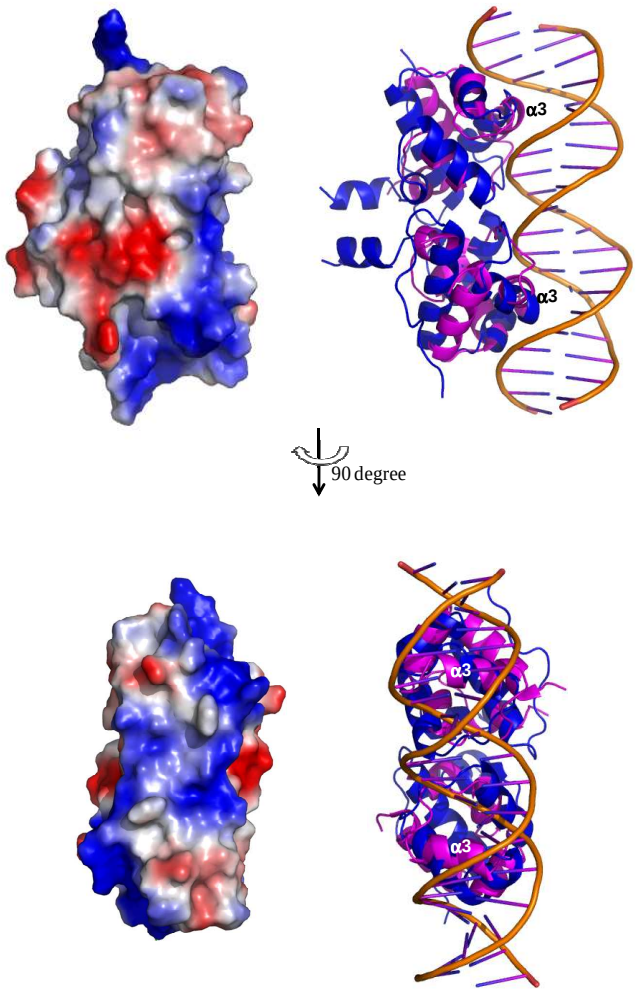

Figure S5

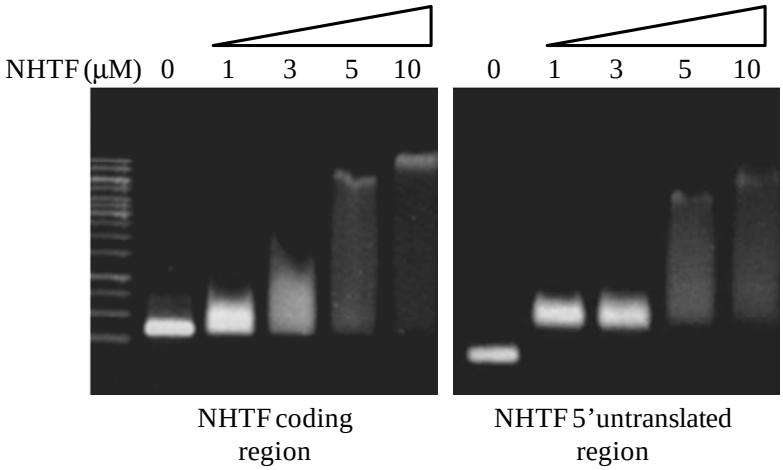
NHTF (μM) 0 1 3 5 10
0 1 3 5 10
NHTF coding region
NHTF 5'untranslated region

Figure S6

T7 promoter Lac operator NHTF binding site

AGATCTCGATCCCGCGAAATTAATACGACTCACTATAGGGGAATTGTGAGCGGATAACAATTCCCCTTATGTGAAGTA

RBS GFP

AAATCCGTAACAGCAAATAATTTTGTTTAACTTTAAGAAGGAGATATACCATGAGTAAAGGAGAAGAACTTTTCACTG
GAGTTGTCCCAATTCTTGTTGAATTAGATGGTGATGTTAATGGGCACAAATTTTCTGTCAGTGGAGAGGGTGAAGGTG
ATGCAACATACGGAAAACTTACCCTTAAATTTATTTGCACTACTGGAAAACTACCTGTTCCATGGCCAACACTTGTCA
CTACTTTCTCTTATGGTGTTCAATGCTTTTCCCGTTATCCGGATCATATGAAACGGCATGACTTTTTCAAGAGTGCCA
TGCCCGAAGGTTATGTACAGGAACGCACTATATCTTTCAAAGATGACGGGAACTACAAGACGCGTGCTGAAGTCAAGT
TTGAAGGTGATACCCTTGTTAATCGTATCGAGTTAAAAGGTATTGATTTTAAAGAAGATGGAAACATTCTCGGACACA
AACTCGAGTACAACTATAACTCACACAATGTATACATCACGGCAGACAAACAAAAGAATGGAATCAAAGCTAACTTCA
AAATTCGCCACAACATTGAAGATGGATCCGTTCAACTAGCAGACCATTATCAACAAAATACTCCAATTGGCGATGGCC
CTGTCCTTTTACCAGACAACCATTACCTGTCGACACAATCTGCCCTTTCGAAAGATCCCAACGAAAAGCGTGACCACA

His-tag

TGGTCCTTCTTGAGTTTGTAACTGCTGCTGGGATTACACATGGCATGGATGAGCTCTACAAACACCACCACCACCACC

ACTGAGATCCGGCTGCTAACAAAGCCCGAAAGGAAGCTGAGTTGGCTGCTGCCACCGCTGAGCAATAACTAGCATAAC

T7-terminator

CCCTTGGGGCCTCTAAACGGGTCTTGAGGGGTTTTTTGCTGAAAGGAGGAACTATATCCGGAT

Figure S7

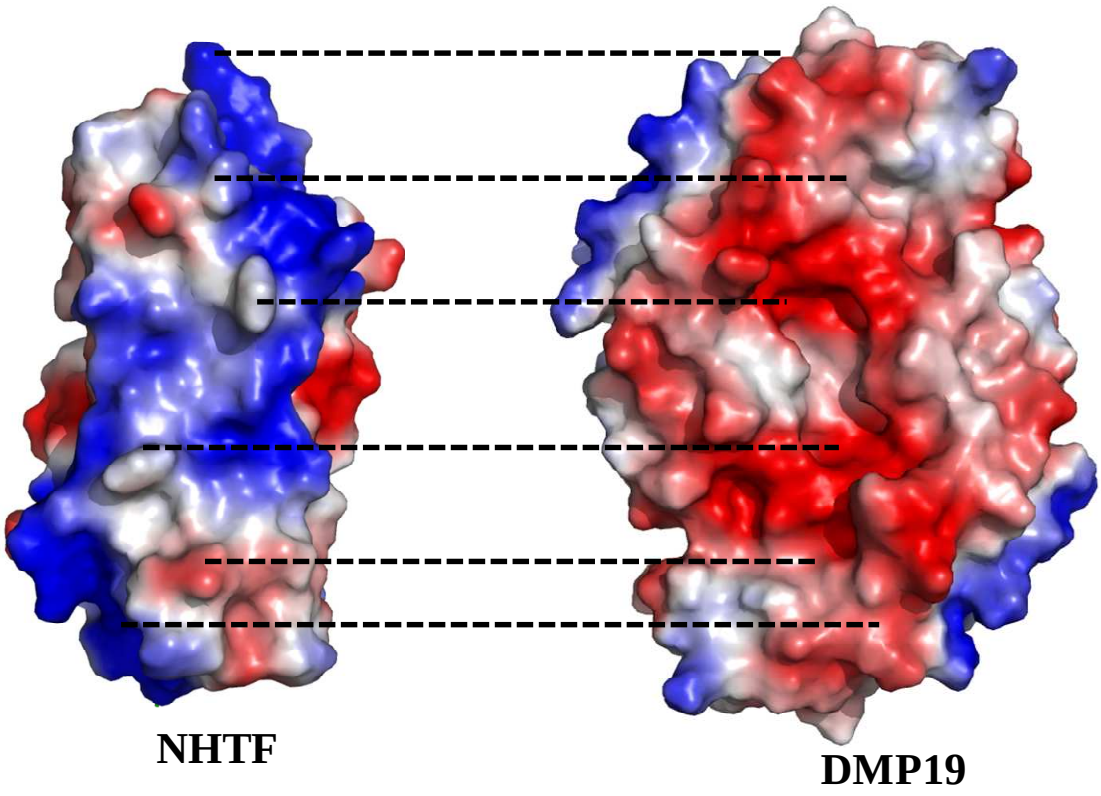

Figure S8